JET–P(98)01

# The Scaling of the Edge Electron Temperature at the L-H Transition based on the Alfvén Drift-Wave Instability

J G Cordey, W Kerner, O Pogutse,
Yu Igitkhanov[1], G Janeschitz[1].

JET Joint Undertaking, Abingdon, Oxfordshire, OX14 3EA,

[1]ITER Joint Central Team, Joint Work Site, D-85748 Garching, Germany.

Preprint of a Paper to be submitted to
Plasma Physics and Controlled Fusion

January 1998

**ABSTRACT**

The stability theory of Alfven drift-waves shows that with increasing plasma pressure the Alfven waves get coupled to electron drift waves. This instability can be characterised by two significant parameters, i.e. the normalised plasma beta and the normalised collision frequency. The resulting turbulent transport coefficient is suppressed when the normalised beta is greater than a critical value, i.e. $\beta_n > 1 + \nu_n^{2/3}$ **,** which depend on the normalised collision frequency $\nu_n$. The transport coefficients change their dependence on plasma parameters at this threshold. The Alfven drift-wave model predicts the scaling of the electron edge temperature at the L-H transition with respect to the toroidal field, plasma current, density and other plasma parameters. The experimental data corresponding to the L-H transition on different tokamaks exhibit a similar behaviour in the $T_0$ - $n_0$ diagram, in particular a weak dependence of $T_0$ on the density at high densities but a more pronounced increase at low densities.

## 1. INTRODUCTION.

Tokamak plasmas experience transition to higher confinement regimes ( the H-mode as discovered first on ASDEX [1] ) when the heating power exceeds a threshold. The explanation of the L-H transition as well as of the power threshold is still incomplete in spite of extensive experimental and theoretical efforts. A comprehensive overview on L-H transition theories is given in Ref. [2] (see in addition references therein), e.g. bifurcation in the electric field, fast ion orbit loss and sheared flow stabilisation. A theoretical model, which describes the L-H transition by the interaction between sheared plasma flow and plasma turbulence, has been discussed in Ref. [3], while the analogous system of model equations has been presented in Ref. [4] for the SOL region. No theory so far has been found to describe the experimental data satisfactorily.

The detailed measurement of the electron edge temperature $T_{0e}$ and density $n_0$, which are now routinely available on many devices [5-10], indicate that there is an ideal MHD beta ( the ratio of plasma pressure to magnetic pressure) threshold for the onset of Giant Edge Localised Modes (ELM's) and furthermore, suggest the existence of a second beta threshold below the ideal ballooning limit for the L-H transition. These data have let to the development of a localised plasma edge physics model. This local analysis model is less involved than the conventional global model for the L-H transition.

The new evidence suggests that the Alfven drift-wave instability [11 - 12] can play an essential role in the edge plasma dynamics. For this instability, as was found many years ago [13], the growth rate for perturbations with a wave number $k_\perp \rho_i \sim 1$ decreases when the plasma beta exceeds the threshold given by the mass ratio of electrons and ions, i.e. $\beta > m_e/M_i$. The transport in the central region of the tokamak plasma is usually related to Ion Temperature Gradient (ITG) modes. However, there is strong experimental evidence that the core plasma instabilities change into electron drift modes near the plasma edge [14]. This makes the

existence of an electron drift- type mode near the plasma edge very plausible; in particular, the Alfven drift- wave instability is of this type. The linear stability theory [13] shows that with increasing plasma pressure the Alfven waves mix with electron drift waves and suppress the unstable long wavelength perturbations, which are dominant in the transport. However, in the non-linear numerical simulations [11], [15 - 17] different qualitative results have been reported. It is, therefore, necessary to proceed with an investigation of the scaling properties of the relevant linear and non-linear equations. Such an analytic approach complements the numerical calculations. It is shown that the scaling can be derived from both the linear and non-linear equations.

Since a tokamak plasma is not expected to be stable against all linear and non-linear modes, the averaged particle and heat flux induced by such instabilities need to be studied. In the stability analysis we do not evaluate the growth rates and eigenfunctions of infinitesimal, linearised perturbations but follow the evolution of finite-amplitude perturbations. Such a (well-known) wave-packet analysis [18] yields the necessary condition for stability. Whereas linear drift waves can be stabilised by magnetic shear, it has been demonstrated by the works of Ref. [19 - 22] that the linearly stable modes can be destabilised nonlinearly and the entire wave-number spectrum gives positive growth rates. Recent numerical simulations [11, 23] also show the existence of these unstable perturbations. Consequently, the assumption for the existence of finite-amplitude Alfven drift-wave perturbations is justified in our analysis. The drive for these finite-amplitude perturbations can be generated by trapped particles, temperature gradients or by a microturbulence background. The increase or decay of the amplitudes of these wave packets and the dependence of the relevant physical parameters is derived.

In this work we combine the dimensional analysis together with the quasilinear approach and derive an expression for the density and energy fluxes based on the Alfven drift-wave instability. The preliminary investigation shows [12] that this instability can be characterised by two dimensional parameters: the normalised plasma beta, $\beta_n = \frac{\beta_0}{\mu} = \left(\frac{M_i}{m_e}\right)^{1/2} \frac{4\pi n_0 T_{0e}}{B_o^2} \frac{1}{k_\parallel x_{0p}}$, and the normalised collision frequency $\nu_n = \frac{\nu}{\sqrt{\mu}} = \left(\frac{M_i}{m_e}\right)^{1/4} \frac{x_{0p}^{1/2}}{\lambda_e k_{||}^{1/2}}$. Here $B_0$ is the toroidal magnetic field, $x_{0p} = -(1/\, p_0 \cdot dp_0 / \, dx)^{-1}$ characterises the pressure gradient scale length and $\lambda_e$ the mean free path and $k_{||}$ is the parallel wave number ($k_{||} \sim s/qR$, where s is the shear of the magnetic field $s=rdq/qdr$ and q the safety factor). All quantities are taken near ( just inside ) the separatrix. The analysis of the transport coefficients shows that the turbulent transport is suppressed when the plasma beta exceeds a critical value, namely $\beta_n > 1 + \nu_n^{3/2}$. This yields the scaling for the edge temperature at the L -H transition in the form $T_{0eV} = K_T s^{a_s} \frac{B_0^{a_B} I_{0M}^{a_I}}{A^{a_A} n_0^{a_n}}$ where all exponents are of

order unity and depend only weakly on the plasma parameters (the exact expression is presented in section 4). The Alfven drift-wave model predicts the correct dependence of the electron edge temperature on density, toroidal field and current [12], [24]. Moreover the scaling for the L - H power threshold found in the recent JET [25] tritium experiments correlates with the mass dependence predicted by our theory.

In Section 2 we derive the quasilinear density and energy fluxes for the electromagnetic case when magnetic field perturbations are essential. Section 3 contains the solution of the dispersion relation and the analysis of the transport coefficient for the Alfven drift-wave instability. In Section 4 the dimensional parameters, which define the L - H transition, are presented and on this basis the scaling for the edge temperature is derived. Section 5 contains the comparison of the theoretical results with experimental evidence from different tokamaks. Section 6 gives the summary of the results. In Appendix I the derivation of the dispersion relation is presented. Appendix II describes the model used for the temperature profile. Finally, Appendix III contains expressions of derived parameters in practical units.

## 2. THE QUASILINEAR DENSITY AND ENERGY FLUXES FOR THE ALFVEN DRIFT - WAVE INSTABILITY.

### a. The quasilinear fluxes in the electrostatic approximation.

The expressions for the quasilinear fluxes in the electrostatic approximation, where the magnetic perturbations are not important, are well known and are, therefore, only briefly discussed here. The turbulent density flux can be obtained from the averaged electron density equation:

$$\frac{\partial}{\partial t}\langle n_e \rangle + div\left(\langle n_e \vec{v}_e \rangle\right) = S_e . \tag{2.1}$$

with the expression for the transverse electron velocity:

$$\vec{v}_{e\perp} = \frac{c}{B_0^2}\left[\vec{B} \times \left(\nabla\varphi + \frac{\nabla p_e}{en}\right)\right]. \tag{2.2}$$

It is easily seen that the diamagnetic part of the velocity does not contribute to the turbulent transport flux when the curvature correction in the magnetic field is not taken into account. Thus, only the E×B part of the velocity is essential for transport. Introducing a slab model in the narrow plasma layer near the separatrix with x as the radial co-ordinate we can write:

$$\frac{\partial}{\partial t} n_0 + \frac{\partial}{\partial x}\left(\Gamma_x\right) = S_e , \tag{2.3}$$

where the particle flux $\Gamma_x$ is

$$\Gamma_x = \langle n' v'_x \rangle = -n_0 \frac{cT_{0e}}{eB_0} \sum_k \mathrm{Re}\left\langle ik_y \tilde{n}_k^* \tilde{\varphi}_k \right\rangle. \tag{2.4}$$

The notations are defined in Appendix I. One can simplify this expression by using for n' the ion density expression (A1.2) in the limit k → 0: $\tilde{n}_i = [k/(\Omega \cdot (1+\eta_e))]\tilde{\varphi}$, which yields $\Gamma_x \sim |\tilde{\varphi}|^2$. The radial displacement $\xi_x$ of the plasma element is introduced by the relation $d\tilde{\xi}/dt = \tilde{v}_\perp$:

$$\gamma \xi_x = v_x = k_y \frac{cT_{0e}}{eB_0} \tilde{\varphi}, \tag{2.5}$$

which gives an estimate for the perturbed potential .

Only the irreversible part of the displacement is taken into account, which is proportional to the imaginary part of the frequency γ, i.e. the growth rate instead of the full frequency ω + iγ. From (2.5) it follows:

$$\tilde{\varphi} = \frac{\gamma eB_0}{cT_{0e} k_y} \xi_x = \pi \frac{\mathrm{Im}(\Omega)}{k^2} \frac{\rho_s}{x_{0p}}. \tag{2.6}$$

We further adapt the normalisation from Appendix I: $\gamma = \mathrm{Im}(\Omega) c_s / x_{0p}$, $k = k_\perp \rho_s$ and suppose that the displacement can not exceed the value $\xi_x \le \pi / k_x$ and $k_y \sim k_x \sim k_\perp$. Finally we can rewrite the particle flux in the form:

$$\Gamma_x = D_\perp \frac{n_0}{x_{0p}(1+\eta_e)} \equiv -D_\perp \frac{\partial n_0}{\partial x}. \tag{2.7}$$

Then using the definition (A1.8) the diffusion coefficient is:

$$D_\perp = \chi_{GB} \cdot \overline{\chi}_\perp, \tag{2.8}$$

where $\chi_{GB}$ is the Gyro-Bohm normalisation coefficient:

$$\chi_{GB} = c_s \rho_s \frac{\rho_s}{x_{0p}}. \tag{2.9}$$

The dimensionless transport coefficient in (2.8) is written in the form:

$$\overline{\chi}_\perp = (\chi_{ML\perp} E)_{\max k}. \tag{2.10}$$

Here we introduce the mixing length turbulent coefficient:

$$\overline{\chi}_{ML\perp} = \pi^2 \frac{\mathrm{Im}(\Omega)}{k^2} \tag{2.10a}$$

together with the quasilinear factor:

$$E = \frac{\mathrm{Im}(\Omega)^2}{\mathrm{Re}(\Omega)^2 + \mathrm{Im}(\Omega)^2}. \tag{2.10b}$$

If the growth rate is large enough $\mathrm{Im}(\Omega) \geq \mathrm{Re}(\Omega)$, i.e. in the strong turbulence case, the usual mixing length estimate for the transport coefficient $\overline{\chi}_{\perp} \approx \mathrm{Im}(\Omega)/k^2$ is obtained (here written in dimensional form), otherwise the expression (2.10) has to be used. The quasilinear correction to the transport essentially improves the agreement of the analytical results with the non-linear numerical simulation [26], [27].

We can rewrite the factor (2.10b) in an equivalent but more physical form. Taking the linearised expression of the radial velocity in the electrostatic limit:

$$v'_{ex} = -i \frac{c k_y T_{0e}}{e B_0} \left( \frac{e\varphi'}{T_{0e}} - \frac{n'_e}{n_0} - \frac{T'}{T_{0e}} \right), \tag{2.11}$$

and using the longitudinal component of the Ohm's low (A1.4) the right hand side of (2.11) can be expressed through the longitudinal component of the velocity or the current ($j_{||} = -en_0 v_{||e}$):

$$v'_{ex} = i \frac{c k_y T_{0e}}{e B_0} \mathbf{R} \frac{v'_{||e}}{v_{Te}}. \tag{2.12}$$

Then the longitudinal velocity is expressed through the density and potential using the continuity equation (A1.3) and the density through the potential using the equation (A1.2). Eventually, the following expression for the quasilinear form factor is obtained :

$$M = \mathrm{Im}(\Omega) \cdot \mathrm{Im} \left| k^2 \mathbf{R} \frac{(\Omega + k \,/\, (\tau(1+\eta_e)))}{\mu\Omega} \right|. \tag{2.13}$$

For the electrostatic case the expressions (2.10b) and (2.13) coincide, but for the case with magnetic perturbations only the last expression makes sense. From (2.13) it is seen that the transport is defined by the dissipative effects in the plasma, i.e. the term R.

By averaging the energy MHD equation we can derive the expression for the energy flux. The equation for the averaged energy reads:

$$\frac{3}{2}\frac{\partial}{\partial t}n_0 T_{0e} + \frac{\partial}{\partial x}\left( q_{ex} + \frac{5}{2}T_{0e}\Gamma_x \right) = P_e , \tag{2.14}$$

where $P_e$ is the heating power and the thermal anomalous flux $q_{ex}$ is defined as:

$$q_{ex} = \frac{3}{2}n_0 \left\langle T_e ' v'_x \right\rangle = -\frac{3}{2}n_0 \frac{cT_{0e}}{eB_0}\sum_k \mathrm{Re}\left\langle ik_y \tilde{T}^*_{ek}\tilde{\varphi}_k \right\rangle . \tag{2.15}$$

Using the expression for the perturbed temperature (in the limit $k \to 0$) $\tilde{T}_e = [k\eta_e / (\Omega \cdot (1+\eta_e))]\tilde{\varphi}$ we can rewrite the heat flux in the usual form:

$$q_{ex} = -\kappa_{e\perp}\frac{dT_{0e}}{dx}, \tag{2.16}$$

where the electron thermal conductivity is:

$$\kappa_{e\perp} = \frac{3}{2}n_0 \chi_{GB}\overline{\chi}_\perp . \tag{2.17}$$

**b. The quasilinear fluxes in the perturbed magnetic field.**

The calculation of the density and energy fluxes in the presence of a perturbed magnetic field it is not as simple as for the electrostatic case. Here we follow the qualitative arguments given in Ref. [28]. In the electrostatic case the irreversible part of the plasma displacement is evaluated in the spatially fixed frame. But a plasma is not held fixed in space but is frozen onto the nested magnetic surfaces. When the magnetic field moves, the plasma does move with these surfaces without inducing anomalous transport, which reflects the ideal frozen-in condition. Such motion takes place in the case of ideal ballooning or kink instabilities. In order to calculate the real transport in a slightly dissipative plasma, not the reversible displacement of the plasma elements in space, we have to find the small irreversible difference between the plasma displacement and the displacement of a given magnetic surface. Only this relative motion defines the anomalous fluxes. The corresponding calculation it is not difficult for the collisionless Vlasov equation [29] but more involved than for the MHD equations [30]. However, it is possible to proceed in the following phenomenological way [28]. We start from the electron momentum equation (which can be considered as the Ohm's law):

$$nm_e \frac{d\vec{v}_e}{dt} + \nabla p_e = -en\left( \vec{E} + \frac{1}{c}\left[\vec{v}_e \vec{B}\right] \right) + en\frac{\vec{j}}{\sigma}. \tag{2.18}$$

If we omit the terms with inertia and conductivity then we obtain:

$$\nabla p_e = -en\left(\vec{E} + \frac{1}{c}\left[\vec{v}_e \vec{B}\right]\right). \tag{2.19}$$

which constitutes Ohm's law for an ideal plasma with a Hall current. In this case the frozen-in conditions are conserved and do not allow the plasma to move through the magnetic surfaces. From the equation (2.19) the expression for the radial velocity of the plasma (2.2) follows, which in the linearised form reads:

$$v'_{ex} = -i\frac{ck_y T_{0e}}{eB_0}\left(\frac{e\varphi'}{T_{0e}} - \frac{n'_e}{n_0} - \frac{T'}{T_{0e}}\right). \tag{2.20}$$

This expression shows that the radial component of the velocity it is not zero in spite of the absence of transport. The expression (2.20) is simply the reversible displacement of the plasma in space. In order to derive the displacement of the magnetic surfaces it is sufficient to take into account the longitudinal component of the full equation (2.18). The linearised version of it can be written as (see Appendix I):

$$\left(\frac{e\varphi'}{T_{0e}} - \frac{n'_e}{n_0} - \frac{T'}{T_{0e}} - \frac{\omega - \omega_{*p}}{k_\| c}\frac{eA'_\|}{T_{0e}}\right) = -\mathbf{R}\frac{v'_{\|e}}{v_{Te}}. \tag{2.21}$$

In the right hand side there are the inertia and conductivity terms. If this dissipative term vanishes transport has to be absent. Defining the "velocity" of the magnetic surfaces as

$$v'_{sfx} = -i\frac{ck_y T_{0e}}{eB_0}\frac{\omega - \omega_{*p}}{k_\| c}\frac{eA'_\|}{T_{0e}}, \tag{2.22}$$

then the difference between the plasma velocity (2.20) and the magnetic surface velocity (2.22) is

$$v'_{dx} = v'_{ex} - v'_{sfx} = -i\frac{ck_y T_{0e}}{eB_0}\left(\frac{e\varphi'}{T_{0e}} - \frac{n'_e}{n_0} - \frac{T'}{T_{0e}} - \frac{\omega - \omega_{*p}}{k_\| c}\frac{eA'_\|}{T_{0e}}\right) = i\frac{ck_y T_{0e}}{eB_0}\mathbf{R}\frac{v'_{\|e}}{v_{Te}} \tag{2.23}$$

This expression vanishes for the ideal case (R = 0) and is proportional to the dissipative processes in a nonideal plasma (R ≠ 0). The final expression (2.23) coincides with the expression (2.12) for the electrostatic limit but in the derivation the magnetic displacement need to be subtracted from the total displacement of the plasma.

In conclusion, we can generalise the electrostatic expression for the transport coefficients $D_\perp$ and $\chi_\perp$ by means of the form factor M. (2.13). The density flux is then given by:

$$\Gamma_x = D_\perp \frac{n_0}{x_{0p}(1+\eta_e)} \equiv -D_\perp \frac{\partial n_0}{\partial x}, \tag{2.24}$$

and the energy flux by:

$$q_{ex} = -\kappa_{e\perp} \frac{dT_{0e}}{dx}, \tag{2.25}$$

The transport coefficients assume the form:

$$D_\perp = \chi_{GB} \cdot \overline{\chi}_\perp, \tag{2.26}$$

$$\kappa_{e\perp} = \frac{3}{2} n_0 \chi_{GB} \overline{\chi}_\perp, \tag{2.27}$$

where the dimensionless transport coefficient reads:

$$\overline{\chi}_\perp = (\chi_{ML\perp} \cdot M)_{\max k}, \tag{2.28}$$

with the form factor given by:

$$M = \mathrm{Im}(\Omega) \cdot \mathrm{Im}\left( k^2 \mathbf{R} \frac{(\Omega + k / (\tau(1+\eta_e))}{\mu\Omega} \right). \tag{2.29}$$

It is emphasised that the expression (2.29) coincides with the particular form for the electrostatic transport case (2.13) , but can not be derived for the electromagnetic case without the subtraction of the magnetic fluxes motion. Moreover, the identical form of the equations (2.29) and (2.13) gives additional validity to this result.

## 3. DISPERSION RELATION AND ANALYSIS OF THE TRANSPORT COEFFICIENTS.

### a. Properties of the Dispersion Relation

The dispersion equation for the Alfven drift-wave instability is derived in Appendix I. The final simplified form (A1.13) contains four independent parameters, namely the normalised plasma beta

$$\beta_n = \frac{\beta_0}{\mu} = \left(\frac{M_i}{m_e}\right)^{1/2} \frac{4\pi n_0 T_{0e}}{B_o^2} \frac{1}{k_\parallel x_{0p}}, \tag{3.1}$$

the normalised collision frequency (or mean free path)

$$\nu_n = \frac{\nu}{\sqrt{\mu}} = \left(\frac{M_i}{m_e}\right)^{1/4} \frac{x_{0p}^{1/2}}{\lambda_e k_{||}^{1/2}}, \tag{3.2}$$

where $\lambda_e = v_{Te}/\nu_e$ is the mean free path for the electrons, the ratio of the temperature and density gradients:

$$\eta_e = \frac{d\ln(T_{0e})}{d\ln(n_0)}, \tag{3.3}$$

and the ratio of electron to ion temperature $\tau = T_{0e} / T_{oi}$.

Here the longitudinal wave number $k_{||}$ for the drift wave can be estimated as usual [18]:

$$k_\parallel \approx \frac{s}{qR}, \tag{3.4}$$

The dispersion equation is a polynomial of fifth order containing four parameters. Using the condition $\mu << 1$ and redefining all variables as done in(A1.11) leads to a fourth order equation. This procedure is not trivial and is not equivalent to setting $\mu = 0$ in the initial expressions (A1.10), because the exact dispersion relation is proportional to $\tilde{}$ itself.

The numerical analysis of the dispersion equation (A!.13) leads to the following conclusions:

1. only one root of the four roots is unstable;
2. the unstable perturbations propagate in the diamagnetic electron direction;
3. the real and imaginary part of the unstable root are of order unity in the dimensional variables;
4. the growth rate has a maximum when the normalised transverse wave number is of order unity;
5. the growth rate is strongly suppressed with increasing plasma pressure;
6. the growth rate increases with increasing temperature gradient;
7. the maximum of the growth rate and of the reciprocal wave number decreases with increasing collision frequency inducing an increase of the transport coefficients (see below);

8. the dependence of the maximum growth rate and of the corresponding wave number on the parameters $\eta_e$ and $\tau$ is relatively weak.

**b. Transport coefficients.**

The normalised transport coefficients, which define the diffusion (2.26) and the thermal conduction (2.27), are now evaluated for the Alfven drift-wave instability :

$$\overline{\chi}_\perp = (\overline{\chi}_{\perp k})_{\max k} \equiv \left[ \mathrm{Im}(\Omega)^2 \cdot \mathrm{Im}\left( \mathbf{R} \frac{(\Omega + k / (\tau(1+\eta_e))}{\mu\Omega} \right) \right]_{\max k} . \qquad (3.5)$$

If we express the right hand side of (3.5) through the renormalised values (A1.11) then we obtain:

$$\overline{\chi}_\perp = \frac{1}{\sqrt{\mu}} \overline{\overline{\chi}}_\perp (\beta_n, \nu_n, \eta_e, \tau) , \qquad (3.6)$$

where the factor $\overline{\overline{\chi}}_\perp (\beta_n, \nu_n, \eta_e, \tau)$ in (3.6)

$$\overline{\overline{\chi}}_\perp (\beta_n, \nu_n, \eta_e, \tau) = (\overline{\overline{\chi}}_{\perp k})_{\max k} \equiv \left[ \mathrm{Im}(\Omega_n)^2 \cdot \mathrm{Im}\left( \mathbf{R} \frac{(\Omega_n + k_n / (\tau(1+\eta_e))}{\Omega_n} \right) \right]_{\max k} , \qquad (3.7)$$

is a function of the parameters $\mu_n, \nu_n, \eta_e$ and $\tau$ only. If these parameters are of order unity then the coefficient $\overline{\overline{\chi}}_\perp (\beta_n, \nu_n, \eta_e, \tau)$ is also of order unity. This implies that the physical transport coefficients are larger than the characteristic (local) Gyro - Bohm value $\chi_{GB}$ (2.9) due to the factor $\frac{1}{\sqrt{\mu}}$ in (3.6):

$$D_\perp = \frac{\chi_{GB}}{\sqrt{\mu}} \cdot \overline{\overline{\chi}}_\perp (\beta_n, \nu_n) , \quad \kappa_{e\perp} = \frac{3}{2} n_0 \frac{\chi_{GB}}{\sqrt{\mu}} \overline{\overline{\chi}}_\perp (\beta_n, \nu_n) . \qquad (3.8)$$

The numerical evaluation yields that the expression $\overline{\overline{\chi}}_\perp (\beta_n, \nu_n, \eta_e, \tau)$ depends only weakly on $\eta_e$ and $\tau$ . Therefore, this dependence can be omitted. In Fig. 1 the dimensionless transport coefficient is displayed as a function of the normalised collision frequency (or the normalised mean free path $1/\nu_n = (m_e / M_i)^{1/4} \lambda_e / (x_{0p} qR)^{1/2}$) and the normalised beta. The dependence of $\overline{\overline{\chi}}_\perp (\beta_n, \nu_n, \eta_e, \tau)$ as a function of $\nu_n$ for different beta values is shown in Fig. 2 ; in particular the asymptotic behaviour of $\overline{\overline{\chi}}_\perp$ with respect to of $\nu_n$ and $\beta_n$ is evident. For the case of small beta and high collision frequency the heat conductivity depends on the collisionality, $\overline{\overline{\chi}}_\perp \sim \nu_n^{1/3}$. But

for small beta and low collisionality $\overline{\overline{\chi}}_{\perp} \sim 1$ , i.e. $\overline{\overline{\chi}}_{\perp}$ does not depend on $\nu_n$. For the case of high beta the dependence of $\overline{\overline{\chi}}_{\perp}$ is more complicated as can be seen from Fig. 1. The different asymptotic behaviour of $\overline{\overline{\chi}}_{\perp}$ can be approximated by the expression:

$$\overline{\overline{\chi}} = \nu_{cr}^{1/3} \frac{\left[1+(\nu_n/\nu_{cr})^2\right]^{1/2}}{\left[1/\nu_{cr}^2+(\nu_n/\nu_{cr})^{4/3}\right]^{1/2}}, \tag{3.10}$$

where

$$\nu_{cr} = \frac{1}{(1+\beta_n^2)^{3/2}}. \tag{3.11}$$

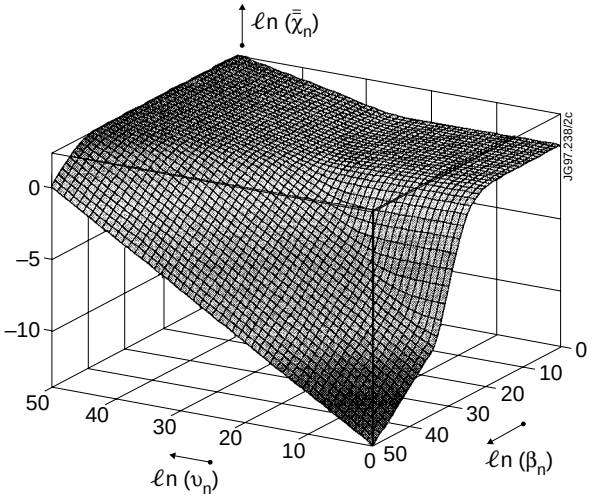


*Fig.1: The surface graphics of the transport coefficient $\chi$.*

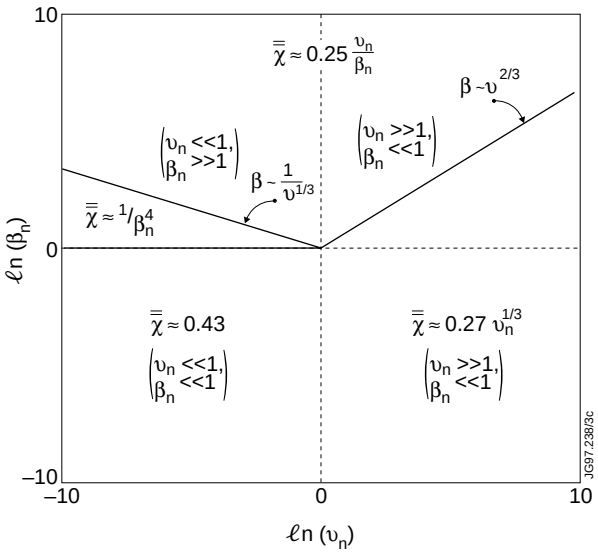


*Fig.2: The asymptotical behaviour of the transport coefficient in the plane (ln($\nu_n$), ln($\beta_n$)). The lines $\beta \sim 1/\nu^{1/3}$ and $\beta \sim \nu^{2/3}$ divide the different asymptotic regions for $\chi$.*

In (3.10) and (3.11) we omit all numerical factors of order unity. This formula approximates the numerical results in all regions in the $(\nu_n, \beta_n)$ plane as can be seen from Fig. 2

The analysis of the turbulent transport coefficient (3.10) give the basic result that the transport decreases when

$$\beta_n > 1 + \nu_n^{2/3}. \tag{3.12}$$

This condition yields the scaling for the edge temperature at the L -H transition. The result (3.12) can be obtained from the following simple consideration. In a low beta plasma ($\beta_0$ <<1 )

the exact expression for the electron density (A1.7) can be expanded in beta:

$$n_e^{'} = n_0 \frac{\left\{\omega_* + i\frac{k_\parallel^2 v_{Te}^2}{\nu_e}\cdot\left[1 + i\frac{(\omega-\omega_*)}{\nu_e\cdot\bar{k}_\perp^2}\cdot\beta_0\right]\right\}}{\left\{\omega + i\frac{k_\parallel^2 v_{Te}^2}{\nu_e}\cdot\left[1 + i\frac{(\omega-\omega_*)}{\nu_e\cdot\bar{k}_\perp^2}\cdot\beta_0\right]\right\}}\frac{e\varphi'}{T_{0e}}. \qquad (3.13)$$

Here $\bar{k}_\perp = k_\perp \cdot \rho_s$. For illustration we take here the simplest case without temperature perturbation and without temperature gradient. If we omit the terms proportional to $\beta_0$ in (3.13) we obtain the electrostatic case. In this limit the dispersion relation contains only one parameters:

$$\Omega^2 + iM\Omega - iM = 0, \qquad (3.14)$$

where $\Omega = \omega/\omega^*$ and $M = \frac{(k_\parallel v_T)^2}{\nu_e} / (\bar{k}_\perp^2 \omega_*)$. In this case the solution of (3.14) can be obtained easily. For the imaginary and real parts of the frequency we have:

$$\gamma = \omega_* \cdot \frac{M^{1/2}}{(1+M^{1/2})^3}, \quad \omega_r = \omega_* \cdot \frac{M^{1/2}}{(1+M^{1/2})}. \qquad (3.15)$$

We again omit here all numerical factors of order unity. From this expression it is easy to see that the mixing length transport coefficient

$$\chi_\perp = \frac{\gamma}{k_\perp^2} = \chi_{GB} \cdot \frac{M^{1/2}}{\bar{k}_\perp (1+M^{1/2})^3} \qquad (3.16)$$

has a maximum in $k_\perp$ for M ~ 1, i.e. for

$$k_\perp \rho_s = \bar{k}_0 \equiv \left[\left(\frac{M_i}{m_e}\right)^{1/2} k_\parallel^2 \lambda_e x_0\right]^{1/3}. \qquad (3.17)$$

Consequently, the maximum value of the heat transport in the electrostatic regime is given by:

$$\chi_\perp = \chi_{GB} / \bar{k}_0. \qquad (3.18)$$

From the expression for the electron density (3.13) we can now estimate when the plasma beta becomes important. This is the case when the second term in the bracket in equation (3.13)

is approximately equal to or greater than unity, i.e. $\frac{(\omega - \omega_*)}{\nu_e \cdot \bar{k}_\perp^2} \cdot \beta_0 > 1$. Taking into account that for M ~ 1 the terms $\gamma$ and $\omega_r$ are in the order of the drift frequency $\omega_*$ this condition can be rewritten as:

$$\beta_0 > \nu_e \cdot \bar{k}_\perp^2 / \omega_* = \left( \frac{M_i}{m_e} \frac{k_\parallel \cdot x_0^2}{\lambda_e} \right)^{2/3} . \qquad (3.19)$$

This result coincides with the condition (3.12) $\beta_n > \nu_n^{2/3}$ in the collisional limit. Using the same considerations for the collisionless case $\omega > \nu_e$, we can derive the condition $\beta_n > 1$, when the electromagnetic effects begin to influence the transport

## 4. EDGE TEMPERATURE SAILING FOR THE L - H TRANSITION.

The previous results make the derivation of the scaling of the electron temperature at the L - H transition feasible. In the early phase of the discharge the plasma is in the L mode. The transport processes inside the plasma column can be divided schematically into the core plasma transport, which is not discussed here but is taken as an experimental fact, and the plasma edge transport, which is dominated in the L mode by the by an electron drift-type instability, such as the Alfven drift-wave instability. Such electron drift instabilities are dominant near the plasma boundary because of the low temperature and high collisionality. The analysis of the previous section shows (3.12) that the turbulence caused transport fluxes decrease when

$$\beta_n > 1 + \nu_n^{2/3}.$$

This condition yields the scaling for the edge temperature at the L -H transition. The estimate of the gradient scale length inside the separatrix $x_0$ is derived from the assumption that the turbulent transport coefficients are continuous across the separatrix and that the convection (collisionless plasma) or conduction (collisional plasma) model in the SOL applies ( see Appendices II and III ).The energy flux from the plasma centre

$$q_{0x} \sim \chi_0 \frac{\bar{T}}{a} \sim \frac{a\bar{T}}{\tau_E} \sim a \frac{p}{n_0}, \qquad (4.1)$$

has to cross the boundary. In (4.1) $\chi_0$ denotes the thermal conduction of the core plasma, $\bar{T}$ is the average plasma temperature, a the small radius, p is the average heating power density p= P/ V, where P is total plasma heating power and V the plasma volume.

For the scrape-off layer plasma ( SOL ) we can use the analogous expression

$$q_x \sim \chi_\perp \frac{T_0}{x_0} \sim q_{0x} \sim a\frac{p}{n_0}. \tag{4.2}$$

Here $\chi_\perp$ is the transport coefficient in the SOL, $T_0$ the temperature at the separatrix (or at the boundary between main plasma and the plasma in the shadow of the limiter ). Using the expression (A2.7) for $x_0$ and assuming continuous transport coefficients across the separatrix we obtain:

$$x_0 \equiv \Delta_s = \sqrt{\chi_\perp \tau_{||}} \tag{4.3}$$

Inserting the results from Appendix II the length $x_0$ can be rewritten as a function of the temperature on the separatrix $T_0$ . Furthermore, the temperature inside the separatrix is approximated by**:**

$$T(a-\Delta x) = T_0 \cdot \left(1 + \Delta x / x_0\right) \approx T_0 \cdot \Delta x / x_0 \quad ; \tag{4.4}$$

$\Delta x$ is the distance inside the plasma from the separatrix to the magnetic surface, where the temperature is measured. Using this expression for $x_0$ as a function of $T_0$ and the condition for the threshold (4.1) the scaling of the temperature at the L - H transition at some distance away from the separatrix T(a-$\Delta x$) with plasma parameters is derived.

In the collisional case $\nu_n > 1$ the following result is obtained:

$$T_{eV}(a-\Delta x) = 32.6 \cdot A^{-1/5} s^{3/5} n_{019}^{-3/10} B_{0T}^{3/5} I_{MA}^{3/5} a_M^{-6/5} \cdot \Delta x_{cm} \text{ (theory).}$$

This result can be compared with the experimental result from ASDEX-UPGRADE :

$$T_e^{crit}(a-2cm) = 145 n_e^{-0.3^{\pm 0.2}_{\pm 0.1}} B_t^{0.8^{\pm 0.2}_{\pm 0.1}} I_p^{0.5^{\pm 0.2}_{\pm 0.2}} \left[eV\right] \text{ (ASDEX [9]).}$$

The theoretical dimensional scaling is found to agree well with the experimental scaling In addition, the numerical coefficient agrees up to a factor of two with the experimental data for $\Delta x_{cm} = 2cm$

For the collisionless case $\nu_n < 1$ the estimate holds :

$$T_{eV}(a-\Delta x) = 23.3 \cdot A^{-1/2} s n_{019}^{-1} B_{0T} I_{MA} a_M^{-2} \cdot \Delta x_{cm}$$

The general expression for $T_{eV}$ for arbitrary collisionality $\nu_n$ can be expressed in the following interpolating form:

$$T_{eV}(a-\Delta x) = c_T \frac{f3\cdot A^{-0.5 f1}}{n_{019}^{f2}} \left( \frac{s \cdot B_{0T} \cdot I_{MA}}{a_M^2} \right)^{f4} \cdot \Delta x_{cm}, \qquad (4.5)$$

where $f1 = (1+2/5\cdot\nu1)/(1+\nu1)$, $f2 = (1+3/10\cdot\nu1)/(1+\nu1)$, $f3 = (1+\nu1)/(1+7/10\cdot\nu1)$, $f4 = (1+3/5\cdot\nu1)/(1+\nu1)$ and $\nu1 = \left(n_{019}/n_{cr}\right)^{21/10}$, $n_{cr} = \left(B_{0T}\cdot I_{MA}/BI\right)^{4/7}$, $BI = c_{BI} A^{3/7} s^{-4/7} a_{0M}^{8/7} Z_{eff}^{2/7}$. This formula contains two additional parameters $c_T$ and $c_{BI}$. Theory gives the values $c_T$=23.3 and $c_{BI}$=1.4. The fit with the ASDEX data yields $c_T$=10 and $c_{BI}$=0.7. The constants are now fixed at the experimental values from ASDEX and held constant in the application to the results from all other tokamaks. The comparison of the theoretical predictions with the experimental findings is displayed in the Figs. 3-7 and is described in detail in the next section.

## 5. COMPARISON WITH TOKAMAK EXPERIMENTS.

We summarise here our understanding of the physical processes involved. In the core plasma the transport scales like Gyro-Bohm, which is in agreement with the dominance of ion temperature gradient modes. Near the plasma edge the transport is more consistent with a Bohm-like scaling suggesting that electron drift waves are involved. For example in the collisional case the transport coefficient (3.8) (or (3.18)) scales as $\chi \propto \frac{1}{q^{2/5}} \frac{T_e^{3/2}}{n_0^{1/5} B_0^{6/5}}$, if we express the edge length scale $x_0$ through the plasma parameters. Consequently, it is assumed that electron drift waves dominate the transport at the edge. The level of transport then depends on the local beta value. With increasing plasma pressure the electron drift waves couple with Alfven waves according to linear theory [13]. As a consequence the unstable long wavelength perturbations which are the most important for transport at the edge are suppressed. The threshold condition on beta can be characterised in terms of two dimensionless normalised parameters: the plasma beta $\beta_n = \frac{\beta_0}{\mu} = \left(\frac{M_i}{m_e}\right)^{1/2} \frac{4\pi n_0 T_{0e}}{B_o^2} \frac{1}{k_\parallel x_{0p}}$ and the collision frequency $\nu_n = \frac{\nu}{\sqrt{\mu}} = \left(\frac{M_i}{m_e}\right)^{1/4} \frac{x_{0p}^{1/2}}{\lambda_e k_{||}^{1/2}}$ being functions of the local plasma parameters. In a collisionless plasma the turbulent transport coefficient starts to decrease for $\beta_n > 1$. This yields a scaling for the edge temperature at the L-H transition of the form $T_{0edge} \sim B_{0T} I_{MA} n_0^{-1}$. For the collisional case the turbulent transport decreases for $\beta_n > \nu_n^{2/3}$. This leads to the scaling for $T_0$ of the form $T_{0edge} \sim B_{0T}^{0.6} I_{MA}^{0.6} n_0^{-0.3}$. For both limits the estimate of gradient scale length $x_0$ is derived by assuming that the turbulent transport coefficients are continuous across the separatrix and that the characteristic time for parallel transport in the SOL is due to electron conduction along the open field lines. This Alfven

drift-wave instability model predicts a close to linear dependence of the edge temperature on the toroidal field. The edge temperature at the threshold rises strongly with density at low densities where the edge plasma is collisionless, and has only a weak dependence at high densities where the plasma is collisional. The experimental points corresponding to the L - H transition in different tokamaks reveal a similar behaviour in the $n_0 - T_{0e}$ diagram. The temperature at the on-set of the Alfven-drift instability is plotted against the plasma density in $n_{boundary}$ - $T_{boundary}$ space (see ITER memo [31] ) for different machines and compared with experimental data points (see Fig. 3 - 7). The width of the H-mode transport barrier, $x_0$, is assessed from the radial profiles. The coefficients in our model has been calibrated to match the L-H transition points for ASDEX-UP ( collisional case ) and then kept constant in the application to other tokamaks as well as in the extrapolation to ITER. Shown in Fig. 3 is the operational space for ASDEX Upgrade in terms of $n_e$ and $T_e$ at r = a – 2cm for constant magnetic field. The magnetic shear near the separatrix has the value s=3. The squares correspond to L - mode data just before transition, whereas the rhombus (◊ ) correspond to the case with type III ELM's in H-mode [8,32]. Similar transition points, i.e. early H- mode data just after transition, are shown for DIIID in Fig.4.

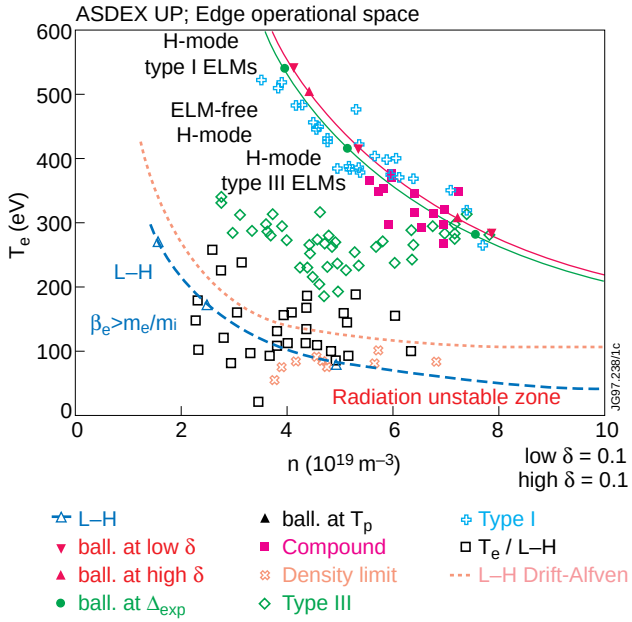


*Fig.3: Operational space diagram (n-Te at 2 cm from separatrix) for L-H transitions in ASDEX Up; experimental points are L-mode regimes just before transition [5,6]; above the dotted line drift-Alfven perturbation are stabilised; shear at the separatrix s=3; dashed line corresponds the condition $\beta_e = m_e/M_i$.*

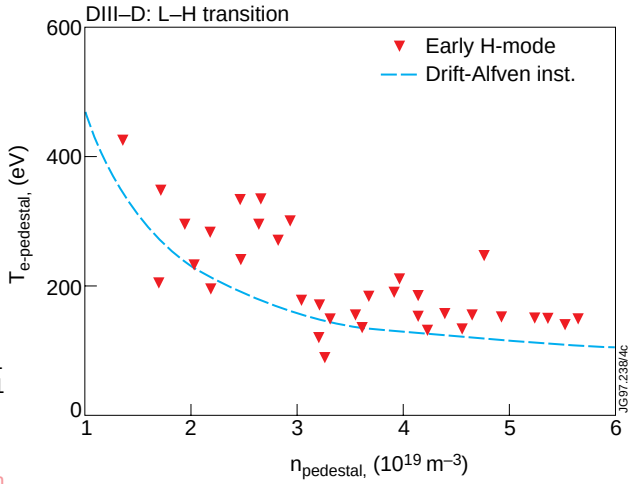


*Fig.4: The same as in Fig.1 for DIII-D; experimental points are H-mode regimes just after transition ; above the rigid line drift-Alfven perturbation is stabilised; $x_0$ = 7cm, shear value at the separatrix s = 5, dashed line corresponds s = 3.*

The data refer to $q_{95}$ = 3.9, $x_0$ = 2cm and a shear value at the separatrix s = 3 [6,7]. In both tokamaks the predictions from our theory are in good agreement with the experimental data, in particular the asymptotic behaviour al high and low density. In FIG. 3 ( showing the data from ASDEX-UP), the limit $\beta_e > m_e / M_i$, which indicates the coupling of electron drift waves with

Alfven waves, is also indicated. This limit corresponds to instabilities with $k_\wedge r_i \sim 1$ which are in general not the most unstable perturbations. It is evident from FIG. 3 that the Alfven drift-wave model does fit the data better. The dependence of the edge temperature on the magnetic field for ASDEX discharges with 1 MA current is displayed in FIG. 5. The theoretical scaling exhibits good agreement with the experimental data. Note that there is some variation in density. The final comparison is performed with results obtained at ALCATOR C-MOD at low field ( 5.3 T ) and at high field ( 8 T ), see figures 6 and 7. In both cases the plasma current is the same, I = 1MA. The agreement of the model with the data is good. Again the limit $\beta_e > m_e / M_i$ gives an inconsistent description. The results from JET and JT-60U exhibit agreement with our model, as was shown in Ref [12]. The spread in the discharge parameters is not sufficiently large to derive new information beyond that presented in the diagrams of [12].

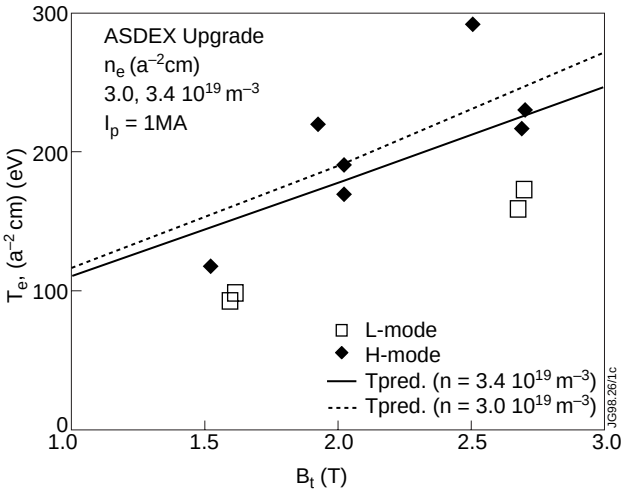


*Fig.5: Dependence of $T_e$(r = a - 2cm) on $B_t$. Shown are discharges with $I_p$ = 1MA and $n_e$(r = a - 2cm) = 3.0… 3.4 $10^{19}m^{-3}$. The dashed curves indicate that $T_{predicted}$ calculated for the different edge densities (3 $10^{19}m^{-3}$ and 3.4 $10^{19}m^{-3}$) increases with increasing $B_t$. $T_{exp}$ corresponds to the best fit to 1996 ASDEX Up data: 145 $n^{-0.3}$ $B^{0.8}$ $I^{0.5}$ (eV, $10^{19}m^{-3}$, T, MA).*

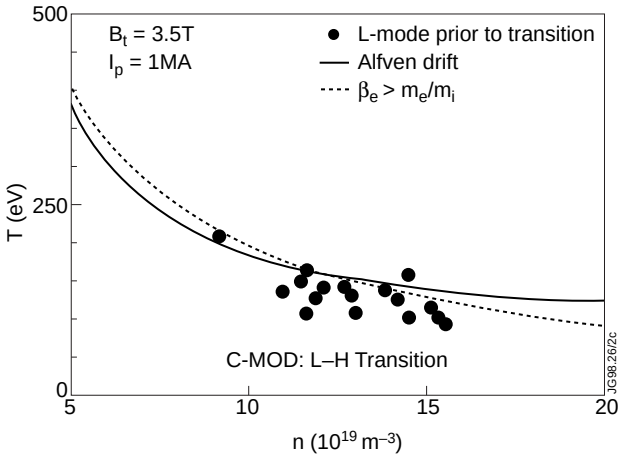


*Fig.6: L - H transition for C - MOD low - B case. Points refer to regimes just prior transition. Pedestal width $\Delta_{exp}$ = 0.8cm. Shear value s = 3.*

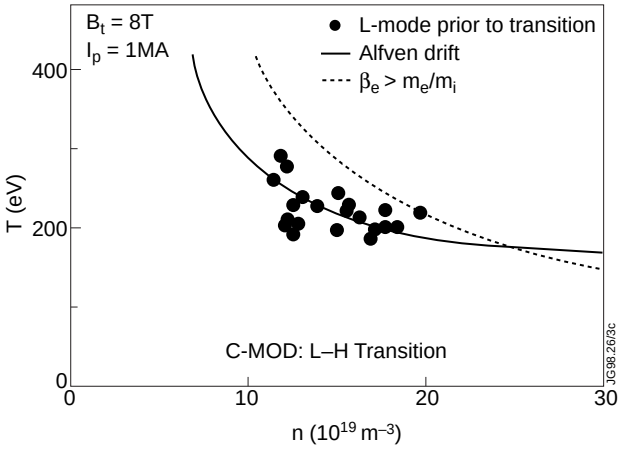


*Fig.7: L - H transition for C - MOD high - B case. Points refer to regimes just prior transition. Pedestal width $\Delta_{exp}$ = 0.8cm. Shear value s = 3.*

## 6. CONCLUSIONS.

The interpretation of the H-mode physics within our model requires stabilisation of both electron and ion turbulence for establishing the transport barrier. The electron turbulence is suppressed by the stabilisation of the Alfven drift-wave instability with increasing edge beta. The ion turbulence is stabilised by poloidal rotation shear. In the L- mode plasma the rotation and the electric field are small**.** Therefore**,** the electron turbulence due to the drift Alfven mode is expected to dominate the transport in the edge region. When the heating power is increased the temperature at the edge increases, the electric field increases slightly, but no pronounced effect on transport is expected. Only when the drift Alfven mode is stabilised and thus electron transport is strongly reduced a sudden further increase of the edge temperature and density becomes possible. As a result the region in which a sheared electric field exists becomes wider. This effect enlarges, therefore, the width over which the ion turbulence is stabilised by sheared poloidal rotation. Therefore, the drift Alfven mode acts as an important trigger mechanism, but the H-mode transport barrier develops only in the region where both electron and ion turbulence are stabilised and thus over the width defined by the shear in the poloidal rotation. However, the confinement does improve in the core, too, if the critical temperature gradient for ion turbulence is determined by the boundary condition for the temperature on top of the H-mode pedestal as suggested in.

The comparison of the derived scaling of the electron edge temperature with experiments shows good agreement between theory and data. The dependence at high density ( collisional case ) as well as at low density (collisionless case) is, in particular, reproduced by the data. In addition the magnetic field scaling, which is well established at ASDEX and C-MOD, is well described.

The prediction for ITER based on the drift-Alfven model shows that within typical range of the edge density (2-8 $10^{19}m^{-3}$) the L-H transition temperature is in the range of 2 -0.8 keV. The scaling has attractive features such as an inverse scaling with ion mass. Such a scaling with ion mass was recently observed in the tritium experiments on JET. Another positive signature of the scaling is the Zeff dependence at the transition. Higher Zeff's generally increase edge temperature required to access the H-mode due the increased collision frequency.

The main results of this paper are: **1)** the Alfven drift model predicts that the turbulent transport is suppressed when the condition:$\beta_n > 1 + \nu_n^{2/3}$ is satisfied; **2)** the transport coefficients change their dependence on plasma parameters from $\chi \sim T_0^{3/2}/n_0^{1/5}$ (for $\beta_n < \nu_n^{2/3}$) to $\chi \sim n_0^{4/13}/T_0^{20/13}$ (for $\beta_n > \nu_n^{2/3}$); **3)** the Alfven drift model predicts the edge temperature scaling in agreement with experimental findings.

**APPENDIX I.**

**Derivation of the dispersion relation.**

Kinetic theory, which is appropriate for describing the ion motion in the weakly collisional case, is used for representing the perturbed ion density:

$$n_i' = \frac{e\varphi'}{T_{0i}} \left\langle \left( -1 + \frac{\omega - \hat{\omega}_{*i}}{\omega - k_\parallel v_\parallel} \exp(-z) I_0(z) \right) f_{0i}(v_\parallel) \right\rangle, \qquad \text{(A1.1)}$$

where $\hat{\omega}_{*i}$ is the operator of the drift frequency $\hat{\omega}_{*i} = (cT_{0i}k_y / eB_0)(\partial n_0 / \partial x \cdot \partial / \partial n_0 + \partial T_{0i} / \partial x \cdot \partial / \partial T_{0i})$, $z = (k_\perp \rho_i)^2$, $\rho_i^2 = c^2 M T_{0i} / e^2 B_0^2$ and the bracket $\langle \ldots \rangle$ denotes the average with respect to the longitudinal part of the distribution function. For the case, when $\omega_* \approx k_\parallel c_A$, the term $k_\parallel v_\parallel$, which describes the longitudinal dynamic of ions, is unimportant in (A1.1) and there is solely transverse ion motion. Moreover, the complicated Bissell function dependence can be simplified by applying the Pade approximation: $\exp(-z) I_0(z) \approx 1/(1+z)$, which allows to describe perturbations with a transverse wave length of the order of the ion Larmor radius $k_\perp \rho_i \sim 1$.Then the perturbed ion density (A1.1) can be rewritten in the form:

$$n_i' = \frac{e\varphi'}{T_{0i}} \left( -1 + \frac{\omega - \hat{\omega}_{*i}}{\omega} \cdot \frac{1}{1+z} \right) n_0 . \qquad \text{(A1.2)}$$

The expression for the perturbed electron density can be derived from the electron hydrodynamic equations. The linearised electron density equation reads:

$$\omega \frac{n'_e}{n_0} - \omega_* \frac{e\varphi'}{T_{0e}} = k_\parallel v'_{\parallel e} . \qquad \text{(A1.3)}$$

The parallel component of the electron equation of motion yields:

$$\frac{T'}{T_{0e}} + \frac{n'_e}{n_0} = \frac{e\varphi'}{T_{0e}} - \frac{\omega - \omega_{*p}}{k_\parallel c} \frac{eA'_\parallel}{T_{0e}} + \mathbf{R} \frac{v'_{\parallel e}}{v_{Te}}, \qquad \text{(A1.4)}$$

where the dissipative term is written in the form:

$$\mathbf{R} = \frac{\omega + i\nu_e}{k_\parallel v_{Te}} \quad , \qquad \text{(A1.4a)}$$

where $\nu_e$ is the electron collision frequency.

Ampere's law gives the connection between the perturbed current $j'_{\parallel} = -en_0 v'_{\parallel e}$ and the longitudinal component of the vector potential of the magnetic field $B'_x = ik_y A'_{\parallel}$:

$$k_{\perp}^2 \delta^2 \frac{eA'_{\parallel}}{T_{0e}} = -\frac{cv'_{\parallel e}}{v_{Te}^2}. \qquad \text{(A1.5)}$$

The expression for the temperature perturbation is obtained from the energy equation:

$$(\omega - \frac{k_{\parallel}^2 v_{Te}^2}{\omega + i\nu_e}) \frac{T'}{T_{0e}} - \omega_{*T} \frac{e\varphi'}{T_{0e}} = \frac{2}{3} k_{\parallel} v'_{\parallel e}. \qquad \text{(A1.6)}$$

In this expression the frequency is added in the denominator of the second term in brackets, in analogy to the frequency correction for the conductivity in the last term in (A1.4).

From (A1.3) - (A1.6) the expression for the perturbed electron density is derived, which takes into account both the drift and Alfven type perturbations:

$$n'_e = n_0 \frac{\left\{ \omega_{*-} \frac{(k_{\parallel}^2 v_{Te}^2 k_{\perp}^2 \delta^2)}{\left[\omega - \omega_{*p} + \tilde{\omega} \cdot k_{\perp}^2 \delta^2\right]} \cdot \left[ 1 + \frac{2}{3} \frac{(\omega_* - (3/2)\omega_{*T}) \cdot \tilde{\omega}}{\omega\tilde{\omega} - k_{\parallel}^2 v_{Te}^2} \right] \right\}}{\left\{ \omega_{-} \frac{(k_{\parallel}^2 v_{Te}^2 k_{\perp}^2 \delta^2)}{\left[\omega - \omega_{*p} + \tilde{\omega} \cdot k_{\perp}^2 \delta^2\right]} \cdot \left[ 1 + \frac{2}{3} \frac{\omega \cdot \tilde{\omega}}{\omega\tilde{\omega} - k_{\parallel}^2 v_{Te}^2} \right] \right\}} \frac{e\varphi'}{T_{0e}}. \qquad \text{(A1.7)}$$

Here $\omega_* = -(ck_y T_{0e} / eB_0) \cdot \partial \ln(n_0) / \partial x$, $\omega_{*T} = -(ck_y / eB_0) \cdot \partial T_{0e} / \partial x$, $\omega_{*p} = -(ck_y T_{0e} / eB_0) \cdot \partial \ln(p_0) / \partial x$ are the electron drift frequencies for the density, temperature and pressure gradients, respectively; $k_{\parallel}$ is the longitudinal wave number, $v_{Te} = (T_{0e} / m_e)^{1/2}$ the thermal electron velocity and $\delta = c/\omega_{pe}$ is the collisionless skin length, $\tilde{\omega} = \omega + i\nu_e$. In this paper we are mainly concerned with dimensional analysis, consequently in (A1.7) numerical factors of order unity are neglected and the effect of the thermal force is omitted.

From the quasineutrality condition $n'_e = n'_i$ the dispersion relation for Alfven drift wave instability [13] is derived. It is convenient to rewrite it in dimensional form by introducing the following dimensionless parameter: $x_{0p} = -(\partial \ln(p_0) / \partial x)^{-1}$, which characterises the gradient length for the pressure. The following relation holds between the pressure, density and the temperature gradients:

$$\frac{1}{x_{0p}} = \frac{1}{x_{0n}} + \frac{1}{x_{0T}}. \qquad \text{(A1.8)}$$

We normalise the quantities with respect to the pressure gradient and use the notation $\eta_e = x_{0n}/x_{0T} \equiv d\ln(T_{0e})/d\ln(n_0)$. Thereby, the dimensionless frequency is defined as $\Omega = \omega \cdot x_{0p}/c_s$, where $c_s = (T_e/M_i)^{1/2}$ is the sound speed; the normalised transverse wave number as $k = k_\perp \rho_s$, where $\rho_s$ is the ion Larmor radius for the electron temperature; the normalised longitudinal wave number as $\mu = k_\parallel v_{Te} x_{0p}/c_s$ and $\nu = \nu_e x_0/c_s$ as the normalised electron collision frequency. Then the normalised drift frequencies are defined as $\omega_{*p} x_{0p}/c_s = k_y \rho_s \approx k$ (here we suppose that $k_y$~k), $\omega_* x_{0p}/c_s = k_y \rho_s/(1+\eta_e) \approx k/(1+\eta_e)$ and $\omega_{*T} x_{0p}/c_s = k_y \rho_s \eta_e/(1+\eta_e) \approx k\eta_e/(1+\eta_e)$; furthermore, $\tau = T_{0e}/T_{0i}$ and $\beta_0 = 4\pi n_0 T_{0e}/B_0^2 \cdot (M/m_e)$ is the normalised electron beta.

Then the perturbed ion density assumes the form:

$$\tilde{n}_i = \left( -\tau + \frac{\Omega\tau - k/(1+\eta_e)}{\Omega} \cdot \frac{1}{(1+k^2/\tau)} \right) \tilde{\varphi}, \qquad \text{(A1.9)}$$

where $\tilde{n} = n'_i/n_0$ and $\tilde{\varphi} = e\varphi'/T_{0e}$, and the perturbed electron density the form:

$$\tilde{n}_e = \frac{\dfrac{k}{1+\eta_e} - \dfrac{\mu^2 k^2}{(\Omega - k)\beta_0 + \tilde{\Omega} k^2} \cdot \left[ 1 + \dfrac{2}{3} \dfrac{k\tilde{\Omega}}{\Omega\tilde{\Omega} - \mu^2 k^2} \left( \dfrac{1 - 3/2\eta_e}{1+\eta_e} \right) \right]}{\Omega - \dfrac{\mu^2 k^2}{(\Omega - k)\beta_0 + \tilde{\Omega} k^2} \cdot \left[ 1 + \dfrac{2}{3} \dfrac{\Omega\tilde{\Omega}}{\Omega\tilde{\Omega} - \mu^2 k^2} \right]} \tilde{\varphi}, \qquad \text{(A1.10)}$$

where $\tilde{\Omega} = \Omega + i\nu$.

The dispersion relation, which follows from the quasi neutrality condition $\tilde{n}_e = \tilde{n}_i$, is an algebraic equation of fifth order with complex coefficients containing four independent parameters, namely $\beta_0, \nu, \eta_e, \mu$. Further investigation yields that additional simplification is obtained, if the subsequent renormalization is made by introducing new dimensional variables and parameters:

$$\Omega_n = \Omega/\sqrt{\mu},\ k_n = k/\sqrt{\mu},\ \beta_n = \beta_0/\mu,\ \nu_n = \nu/\sqrt{\mu}. \qquad \text{(A1.11)}$$

Then the transitions between the collisional and the collisionles regimes and between low and high beta plasma occur for $\nu_n$, $\beta_n$, values in the order of unity. The numerical evaluation of the dispersion relation reveals that the new growth rate and frequency depend only weakly on $\mu$

for experimentally relevant small values $\mu < 1$. Consequently, it is consistent to set $\mu = 0$ in the subsequent calculations. This implies that the dispersion relation is reduced to fourth order with three independent parameters:

$$\mu_n, \nu_n, \eta_e. \tag{A1.12}$$

This simplifies the analysis considerably. The dispersion equation in the new variables reads:

$$a4(\beta_n, \nu_n, \eta_e)\Omega_n^4 + a3(\beta_n, \nu_n, \eta_e)\Omega_n^3 + a2(\beta_n, \nu_n, \eta_e)\Omega_n^2 + a1(\beta_n, \nu_n, \eta_e)\Omega_n^1 ;$$

$$^{\llcorner} + a0(\beta_n, \nu_n, \eta_e) = 0 ,$$

where the coefficients are:

$$a4(\beta_n, \nu_n, \eta_e) = \tau(\beta_n + k_n^2);$$

$$a3(\beta_n, \nu_n, \eta_e) = k_n(\beta_n + k_n^2)/(1+\eta_e) + 2i\nu_n k_n^2 \tau - \tau\beta_n k_n + i\nu_n \beta_n \tau; \tag{A1.13}$$

$$a2(\beta_n, \nu_n, \eta_e) = (i\nu_n \beta_n k_n + 2i\nu_n k_n^3 - k_n^2 \beta_n)/(1+\eta_e) - i\nu_n \beta_n k_n \tau - \tau k_n^2 \nu_n^2 - \tau;$$

$$a1(\beta_n, \nu_n, \eta_e) = \tau k_n + (-i\nu_n \beta_n k_n^2 - k_n^3 \nu^2)/(1+\eta_e); \quad a0(\beta_n, \nu_n, \eta_e) = i\tau\nu_n k .$$

## APPENDIX II

### Temperature profile for a simplified transport model.

The radial dependence of the temperature can be approximated by the following simple model. It is assumed that the plasma consists of three regions: a) the central plasma, which extends over the major part (1-Δ) of the plasma radius, with transport coefficient $\chi_0$ and the power heating density per particle $\overline{p} \neq 0$; b) the plasma near the boundary but inside the separatrix of width Δ with the drift type transport coefficient $\chi_1$ and c) the outer separatrix region having the same transverse transport coefficient $\chi_1$ with the longitudinal loss on the characteristic time $\tau_{\|}$; the width of this region is $\Delta_s$ as is detailed below. For simplicity all coefficients are assumed to be constant here ( which does not change the qualitative character of the conclusions ). In this model heat sources are absent in the regions b) and c). Then the radial temperature profile can be expressed as:

a) $$T(x) = T(0) - \frac{1}{2}\frac{\overline{p}}{\chi_0}x^2, \quad (0 \le x < 1-\Delta) \tag{A2.1}$$

where T(0) is the central temperature

$$T(0) = \frac{1}{2}\frac{\overline{p}}{\chi_0}(1-\Delta)^2 + T_t, \tag{A2.2}$$

with

$$T_t = \frac{\overline{p}}{\chi_1}(1-\Delta)(\Delta + \Delta_s); \tag{A2.3}$$

the transition temperature between region a) and b):

b) $$T(x) = \frac{\overline{p}}{\chi_1}(1-\Delta)(1-x+\Delta_s) \equiv \frac{\overline{p}}{\chi_1}(1-\Delta)(1-x) + T_s, \quad (1-\Delta \le x < 1) \tag{A2.4}$$

where $T_s$ is the separatrix temperature

$$T_s = \frac{\overline{p}}{\chi_1}(1-\Delta)\Delta_s; \tag{A2.5}$$

and finally the temperature profile in the SOL region

c) $$T(x) = T_s \exp(-\frac{(x-1)}{\Delta_s}), \quad (1 \le x < \infty) \tag{A2.6}$$

where

$$\Delta_s = \sqrt{\chi_1 \tau_{\parallel}} \tag{A2.7}$$

is the characteristic SOL width.

The temperature just inside the separatrix can be written according to (A2.4) as

$$T(x) = T_s(1+\frac{1-x}{\Delta_s}) = T_s(1+\frac{\Delta x}{\Delta_s}), \tag{A2.8}$$

where $\Delta x = 1 - x$ is the distance from the separatrix inside to plasma. From (A2.4) it is seen that for a distance $\Delta x \le \Delta_s$ the temperature scales as $T_s$ and can be few times greater than $T_s$

$$T \propto T_s \quad (\Delta x \le \Delta_s) \tag{A2.9}$$

and for $\Delta x > \Delta_s$ the temperature scales as $T_s/\Delta_s$.

$$T \propto T_s/\Delta_s \approx T_t \quad (\Delta x > \Delta_s) \tag{A2.10}$$

The quantity $T_{0e}$ as introduced in the main text coincides with $T_s$ and the length $x_0$ with $\Delta_s$.

## APPENDIX III

**Expressions for different plasma parameters in a practical system of units.**

The expressions for important plasma parameters are expressed in practical units. The dimensionless plasma pressure and collision frequency read:

$$\beta_n = 0.86 \cdot 10^{-2}\, A^{1/2}\, \frac{n_{013} T_{0eV}}{B_{0T}^2 x_{0cm} k_{\parallel m}}, \tag{A3.1}$$

$$\nu_n = 3.4 \cdot 10^{2}\, C_z A^{1/4}\, \frac{x_{0cm}^{1/2} n_{013}}{T_{0kV}^2 k_{\parallel m}^{1/2}}, \tag{A3.2}$$

where the factor $C_z$ takes into account that $Z_{eff}$ need not be equal to one.

The transport coefficients have the form for the Gyro-Bohm coefficient

$$\chi_{GB}\left[\frac{cm^2}{\sec}\right] = 10^2\, \frac{A^{1/2} T_{0eV}^{3/2}}{B_{oT}^2 x_{0cm}}\,, \tag{A3.3}$$

and for the transport induced by the Alfven drift-wave instability in the collisional regime for low beta

$$\chi_{\perp}\left[\frac{cm^2}{\sec}\right] = 10^3\, C_{\chi}\, \frac{A^{1/2} T_{0eV}^{3/2} n_{013}^{1/3}}{B_{oT}^2 x_{0cm}^{4/3} k_{\parallel m}^{2/3}}\,, \tag{A3.4}$$

where the numerical factor $C_\chi$ takes into account the difference between the quasilinear estimate and the true value of the transport coefficients. We introduce the additional quantities $C_z$, $C_\chi$, $C_{kL}$ in order to allow a sensitivity check of the final scalings on these not very well known factors. In these expressions A is the atomic number, $n_{013}$ is the density in $10^{13}$cm$^{-3}$ unit, the temperature $T_{0eV}$ is expressed in eV, the main toroidal magnetic field $B_{0T}$ is expressed in Tesla, the characteristic gradient $x_{0cm}$ expressed in cm, the longitudinal wave number $k_{\parallel m}$ is expressed in “m” and reads

$$k_{\parallel m} = C_{kL}\, \frac{s}{q R_m}, \tag{A3.5}$$

where “s” is the shear of the magnetic field s=(adq/qda), q is the cylindrical safety factor

$$q = 5 \frac{a_m^2 B_{0T}}{R_m I_{0M}}, \tag{A3.6}$$

and $C_{kL}$ is the numerical factor which takes into account the existence of the separatrix ($C_{kL}$ ~ 0.3). In (A3.6) $a_m$ is small tokamak radius in "m", $R_m$ is the large radius and $I_{0M}$ the total current in MA.

The longitudinal time loss for the heat conduction regime in the SOL is taken in the form:

$$\tau_{\parallel}^{e}\left[\sec\right]= 1.23\cdot 10^{-3} C_z \frac{n_{013}}{k_{\parallel m}^2 T_{oeV}^{5/2}} \tag{A3.7}$$

and for the convection case

$$\tau_{\parallel}^{e}\left[\sec\right]= 0.36\cdot 5\cdot 10^{-5} \frac{1}{k_{\parallel m} T_{oeV}^{1/2}} \quad . \tag{A3.8}$$

and

$$\lambda_e\left[cm\right]= \frac{0.1}{C_z}\frac{T_{0eV}^2}{n_{013}}. \tag{A3.9}$$

is the electron mean free path.

**REFERENCES**


1. ASDEX team, The H - mode in ASDEX, Nuclear Fusion, 29, 1959 (1989).
2. H.R.Wilson and J.W.Connor, "Theories of the L - H Transition Phenomenon and their Predictions", (to be published).
3. B.A.Carreras *et al*, Proc. 20th EPS conference on Controlled Fusion and Plasma Physics (Lisboa, 1993) vol. 4 (Vienna: IAEA) p. 1419.
4. O.Pogutse *et al*, Plasma Phys. Control. Fusion, 36, 1963 (1994). P.R.Thomas, V.P.Bhatnagar and the JET Team, "JET and the Road to ITER", Preprint JET-P(97)52.
5. P.R. Thomas, V.P. Bhatnagar and the JET Team, "JET and the Road to ITER", Preprint JET-P(97)52.
6. T. Osborne *et al*, "ELM Studies on DIII-D," Bulletin of the American Physical Society APS DPP Meeting, Denver, Nov. 11-15, 1996 (1996).
7. D.M. Thomas *et al*, Bulletin of the American Physical Society, APS DPP Meeting, Denver, Nov. 11-15, 1996 (1996).
8. M. Kaufmann et al, "Overview of ASDEX Upgrade Results," presented at the Sixteenth IAEA Fusion Energy Conference, Montreal, Canada, 1996 IAEA-CN-64/O2-5.
9. W.Suttrop et al, Plasma Phys. Control. Fusion, 39, 2051 (1197).
10. J.G.Cordey and JET Team, Proc. 16th Int. Conf. on Plasma Phys. and Contr. Nucl. Fusion Res. (1996) vol. 1 (Vienna: IAEA) p. 339.

11. B. Scott, S. Camargo, and F. Jenko, “Self-Consistent Computation of Transport by Fluid Drift Turbulence in Tokamak Geometry,” presented at the Sixteenth IAEA Fusion Energy conference, Montreal, Canada, 1996 IAEA-CN-64/D-3-4.
12. O. Pogutse, Yu. Igitkhanov, G. Janeschitz, W. Kerner, and J.G. Cordey, “The Alfven drift - wave instability and the L-H transition in a plasma,” presented at the European Physical Society, Berchtesgaden, Germany, 1997.
13. A. Mikhailovskii, *Theory of Plasma Instabilities* (Consultants Bureau, New York-London, 1974).
14. R.D. Durst, R.J. Fonck, J.S. Kim, S.F. Paul, N. Bretz, C. Bush, Z. Chang and R Hulse, Phys. Rev. Letters, 71, 3135 (1993).
15. B.Scott and F.Jenko, “Three Dimensional Computation of Fluid and Kinetic Drift Alfven Turbulence in Tokamak Geometry”, presented at the European Physical Society, Berchtesgaden, Germany, 1997.
16. A.Zeiler, J.F.Drake, D.Biskamp and P.N.Guzdar, Phys. Plasma, 3, 2951 (1996)).Drake
17. B.N.Rogers and J.K.Drake, Phys. Rev. Letters,79,229 (1997).
18. B.B.Kadsomtsev and O.P.Pogutse, *Reviews of Plasma Physics*, v. 5, 249. Consultant Bureau, New York - London, (1970).
19. S.P.Hirshman and K.Molvig, Phys. Rev. Letters, 42, 648 (1979).
20. K.Molvig, S.P.Hirshman and J.C.Whitson, Phys. Rev. Letters, 43, 582 (1979).
21. W.W.Lee *et. al*, Phys. Rev. Letters, 43, 347 (1979).
22. R.D.Sydora *et. al*, Phys. Rev. Letters, 57, 3269 (1986).
23. A.Zeiler, J.F.Drake and D.Biskamp, Phys. Plasma, 4, 991 (1997).
24. G. Janeschitz, et al, Proc. 24$^{th}$ EPS Conference on Controlled Fusion and Plasma Physics (Berchtesgaden, 1997) vol. 3 (Vienna: IAEA) p. 993.
25. M.Keilhacker and the JET Team, “JET D-T Experiments and their Implications for ITER”, Presented at the 16$^{th}$ Symposium on Fusion Energy (SOFE), (San Diego, USE. 6-10$^{th}$ October 1997); Preprint JET-P(97)55.
26. H.Nordman and J.Weiland, Nucl. Fusion, 29, 251 (1989).
27. G.Hu and J.A.Krommes, Phys. Plasma, 4, 2116 (1997).
28. B.B.Kadomtsev, O.Pogutse and E.Yurchenko, Proc. 9$^{th}$ Int. Conf. on Plasma Phys. and Contr. Nucl. Fusion Res. (Baltimore, 1982) vol. 3 (Vienna: IAEA) p. 67.
29. A.I.Smolyakov and P.N.Yushmanov, Nucl. Fusion, 33, 383 (1993).
30. B.B.Kadomtsev (private communication).
31. Yu.Igitkhanov, M.Sugihara, G.Janeschitz, H.Pacher and D.Post, Internal Memorandum Report No. ITER Memo G 19 MD 1 96-12-12 W 0.1 S 17 MD 1 96-12 12 F 1, 1996.
32. H. Zohm, “Edge localized modes (ELMs),” Plasma Physics and Controlled Fusion 38, 105 (1996).

33. A. Hubbard, J. Goetz, M. Greenwald, I Hutchinson, Y. In, J. Irby, B. Labombard, P. O'Shea, J. Snipes, P. Stek, Y. Takase, S. Wolfe, and Alcator Group, "Local Plasma Parameters and H-mode Threshold in Alcator C-Mod," presented at the Sixteenth IAEA Fusion Energy Conference, Montreal, Canada, 1996 IAEA-CN-64/AP2-11.
34. G.Janeschitz, A.Hubbard, Yu.Igitkhanov, J.Lingertat, T.Osborn, H.D.Pacher, O.P.Pogutse, D.E.Post, M.Shimada, M.Sugihara and W.Suttrop, "ITER operation space in terms of Te and ne at the plasma edge", presented at the European Physical Society, Berchtesgaden, Germany, 1997.